Involvement of Cytoplasmic Factors Regulating the Membrane Orientation of P-Glycoprotein Sequences†

Jian-Ting Zhang*,‡ and Victor Ling§

Department of Physiology and Biophysics, University of Texas Medical Branch, Galveston, Texas 77555-0641, and Division of Molecular and Structural Biology, Department of Medical Biophysics, The Ontario Cancer Institute, University of Toronto, 500 Sherbourne Street, Toronto, Ontario, Canada M4X 1K9

Received November 2, 1994; Revised Manuscript Received May 19, 1995⊗

ABSTRACT: Chinese hamster *pgp1* P-glycoprotein (Pgp) is a membrane transport protein that causes multidrug resistance (MDR) by actively extruding a wide variety of cytotoxic agents out of cells. It may also function as a peptide transporter and as a chloride channel. Previously, we have shown that hamster *pgp1* Pgp is expressed in more than one topological form and that the generation of these structures is modulated by charged amino acids flanking the predicted transmembrane (TM) segments 3 and 4. Different topological structures of Pgp may be involved in different functions. In this study, we examined the role of cytoplasmic components in cell-free translation systems in modulating the topologies of Pgp. By using rabbit reticulocyte lysate (RRL) and wheat germ extract (WGE) expression systems, we showed that WGE contains a soluble, heat-labile, high molecular weight fraction that regulates the membrane topology of truncated Pgp molecules. These results and our previous findings indicate that the membrane topology of a mammalian polytopic membrane protein may be regulated both by the amino acid sequence of the protein and by soluble cytoplasmic component(s). We speculate that Pgp expressed in various cell types may have different topological structures modulated by specific cytoplasmic factors.

P-Glycoprotein (Pgp)[1] is a member of the ATP-binding cassette (ABC) membrane transporter family, which transports a wide variety of substrates (Endicott & Ling, 1989; Higgins, 1992; Gottesman & Pastan, 1993; Childs & Ling, 1994). The human *mdr1* Pgp causes multidrug resistance (MDR) in cancer cells by extruding chemotherapeutic drugs. The Chinese hamster *pgp1* Pgp not only transports cytotoxic agents and causes MDR (Childs & Ling, 1994) but also transports peptides (Sharma *et al.*, 1992) and may be associated with a 40 pS chloride channel (Bear, 1994). Hydropathy analyses of deduced protein sequences suggest that Pgp has 12 predicted transmembrane (TM) segments. However, recent studies using rabbit reticulocyte lysate (RRL) (Zhang & Ling, 1991; Zhang *et al.*, 1993), *Xenopus* oocytes (XO) (Skach *et al.*, 1993), and bacteria (Bibi & Beja, 1994) as expression systems suggest that Pgp may exist in more than one topological form. In addition to the predicted 12-TM structure, alternate structures of Pgp containing only 8 (Zhang *et al.*, 1993) or 10 (Skach & Lingappa, 1994) TM segments have been identified. It has been speculated that the different topological structures of Pgp may be involved in the multiplicity of functions attributed to this protein (Zhang *et al.*, 1993). Most recently, we have shown that the generation of the alternate topology in RRL is dependent on charged amino acids flanking some internal predicted TM segments (Zhang *et al.*, 1995). This type of internal topogenic sequence may dictate the topologies of a wide range of polytopic membrane proteins in mammalian cells, as has been shown in bacteria cells (Gafvelin & von Heijne, 1994).

In the present study, we tested whether factors present in different cell-free translation systems affected the generation of the different topologies of Pgp. We compared topologies of Pgp sequence generated with rabbit reticulocyte lysate (RRL) and with wheat germ extract (WGE) translation systems. We observed that WGE contains one or more heat-labile factors that play a dominant role in determining the topology of the Pgp sequence. These results and our previous findings suggest that the amino acid sequences of Pgp and soluble cytoplasmic fractions contribute to the regulation of Pgp topologies. Therefore, it is possible that, in different cell types, different topological structures of Pgp may predominate depending on the particular cytoplasmic factors expressed.

EXPERIMENTAL PROCEDURES

Materials. pGEM-4z plasmid, SP6 and T7 RNA polymerases, RNasin, ribonucleotides, RQ1 DNase, rabbit reticulocyte lysate, wheat germ extract, and dog pancreatic microsomal membranes were obtained from Promega. [^{35}S]-Methionine and Amplify were purchased from New England Nuclear and Amersham Corp, respectively. The m^{7}G(5′)-ppp(5′)G cap analog was obtained from Pharmacia LKB Biotechnology Inc. Peptide *N*-glycosidase F (PNGase F) and restriction enzymes were obtained from Boehringer Man-

† This work was supported by grants from the National Institutes of Health (CA-64539 (J.T.Z.) and CA-37130 (V.L.)), the John Sealy Memorial Foundation for Biomedical Research (J.T.Z.), and the National Cancer Institute of Canada (V.L.).

* Corresponding author: telephone 409-772-3434; Fax 409-772-3381.

‡ University of Texas Medical Branch.

§ University of Toronto.

⊗ Abstract published in *Advance ACS Abstracts,* July 1, 1995.

[1] Abbreviations: Pgp, P-glycoprotein; MDR, multidrug resistance; ABC, ATP-binding cassette; RRL, rabbit reticulocyte lysate; WGE, wheat germ extract; XO, *Xenopus* oocyte; TM, transmembrane; PNGase F, peptide *N*-glycosidase F; RM, rough microsomes; SRP, signal recognition particle; TMBF, transmembrane-binding factor; ER, endoplasmic reticulum.

0006-2960/95/0434-9159$09.00/0

nheim, New England Biolabs, or Promega. The insoluble trypsin was purchased from Sigma. All other chemicals were obtained from Sigma or Fisher Scientific.

In Vitro Transcription and Translation. About 6 μg of recombinant DNA linearized with *Hind*III was transcribed in the presence of 5 A_{260} units/mL cap analog $m^7G(5')ppp(5')G$ as described previously (Zhang & Ling, 1991). Removal of DNA templates with RQ1 DNase after transcription and purification of RNA transcripts were carried out according to Zhang and Ling (1991). Cell-free translations using rabbit reticulocyte lysate and wheat germ extract were performed as described previously (Zhang & Ling, 1991). Proteolysis/membrane protection assay and limited endoglycosidase treatment were performed as described by Zhang *et al.* (1993). The membrane fraction of translation products was isolated by centrifugation and analyzed using SDS–PAGE and fluorography as described previously (Zhang *et al.*, 1993).

Separation of ribosomes in wheat germ extract from soluble fractions was performed by centrifugation in an air-driven ultracentrifuge for 30 min at 20 psi. The supernatant was transferred into a fresh tube, and the ribosome pellet was rinsed with H_2O. Both supernatant and pellet were centrifuged again for 20 min at 20 psi. The ribosome pellet was resuspended in H_2O to its starting volume. Both the soluble and pellet fractions were divided into two halves, and one half was boiled in H_2O for 2 min. Trypsinization of WGE was performed by treating 20 μL of WGE supernatant with 3.75 units of insoluble trypsin (Sigma) at room temperature for 1 h. The insoluble trypsin was then removed by centrifugation. As a control, 10 μL of WGE supernatant was treated under the same conditions in the absence of trypsin.

The Sephadex G-50 spin column was prepared by packing Sephadex G-50 slurry in a 1 mL syringe by centrifugation, followed by three washes with H_2O and centrifugation. WGE (50 μL) was then loaded onto the column, and the excluded fraction was collected by centrifugation. The column was then washed twice with 50 μL of H_2O each time, and the eluate from each wash was collected by centrifugation.

RESULTS

The First Loop Linking the Predicted TM1 and TM2 of Pgp Is Located in the RM Lumen When Expressed in Both RRL and WGE Systems. Figure 1A shows the two models of hamster *pgp1* Pgp topology deduced from previous studies (Zhang & Ling, 1991; Zhang *et al.*, 1993). Model I is same as was predicted from hydropathy plot analysis. Model II is the alternate topology observed in a rabbit reticulocyte lysate (RRL) expression system. Several truncated cDNA constructs encoding the N-terminal half molecules of Chinese hamster *pgp1* P-glycoprotein have been used to study their topological structures in the RRL system supplemented with dog pancreatic microsomal membranes (RM) (Zhang *et al.*, 1993). Three of these constructs are shown in Figure 1B and will be discussed in this study. The *Xho*I/PGP-N6 transcript encodes the first three predicted TM segments of Pgp and has been used to analyze the membrane orientation of the loop linking the predicted TM1 and TM2 in RRL. We have shown that this loop is located in the RM lumen and is glycosylated (Zhang *et al.*, 1993).

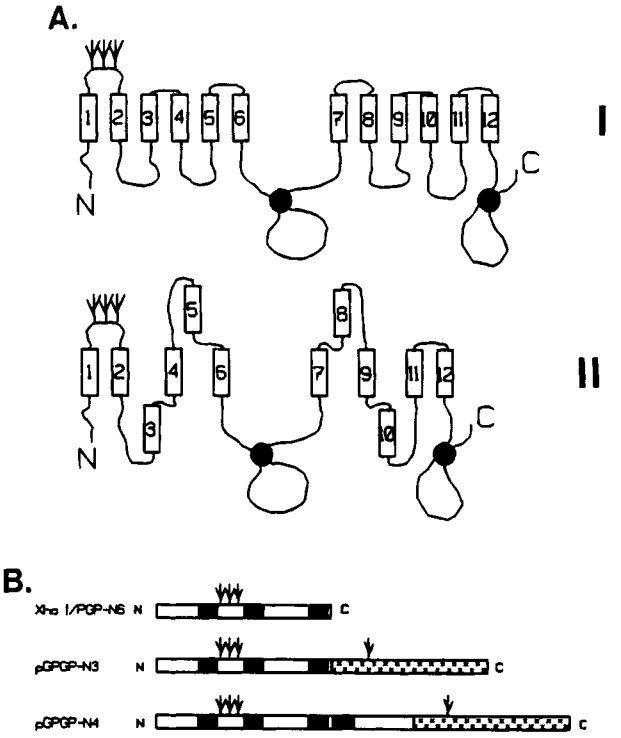

FIGURE 1: (A) Models of the topological structures of P-glycoprotein. Models I and II are deduced from previous studies (Zhang & Ling, 1991; Zhang *et al.*, 1993). Predicted TM segments are shown as open bars numbered sequentially from the N-terminal end. The solid circles and the branched symbols represent ATP-binding sites and N-linked glycosylations, respectively. (B), Schematic diagram of the fusion constructs of hamster *pgp1* Pgp. The solid bars represent the predicted TM segments. The open bars are the nonhydrophobic sequences. The hatched bars represent the reporter peptide. The branched symbols are potential glycosylation sites.

When the *Xho*I/PGP-N6 transcript was used to direct translation in the WGE system supplemented with RM, a protein of 24 kDa associated with the RM fraction was produced (Figure 2A, lane 5), similar to that produced in the RRL system (Figure 2A, lane 1). Treatment with endoglycosidase PNGase F reduced the 24 kDa peptide generated in both systems to ~16 kDa (compare lanes 4 and 8 in Figure 2A). These results suggest that the nascent peptide in the WGE system was also integrated into RM and modified with ~8 kDa oligosaccharides. Although no mammalian signal recognition particle (SRP) was added to the reaction in the WGE system, efficient membrane targeting and translocation of the truncated Pgp were achieved. Possibly, the residual SRP associated with RM is sufficient for membrane targeting and translocation of mammalian proteins in the WGE system (Walter *et al.*, 1981; Meyer *et al.*, 1982; Zhang & Ling, 1991). To show that the loop linking the predicted TM1 and TM2 of this nascent peptide is in the RM lumen and contains oligosaccharide chains, the RM fractions from each translation were treated with proteinase K followed by treatments with PNGase F. Treatment with proteinase K alone generated a major fragment of ~19 kDa in both the RRL (Figure 2A, lane 2) and the WGE systems (Figure 2A, lane 6). Further PNGase F treatment reduced this 19 kDa fragment to ~11 kDa (Figure 2A, lanes 3 and 7), suggesting that the protease-resistant 19 kDa fragment contains all of the ~8 kDa oligosaccharide residues and represents the membrane-protected TM1–loop–TM2 fragment. This is consistent

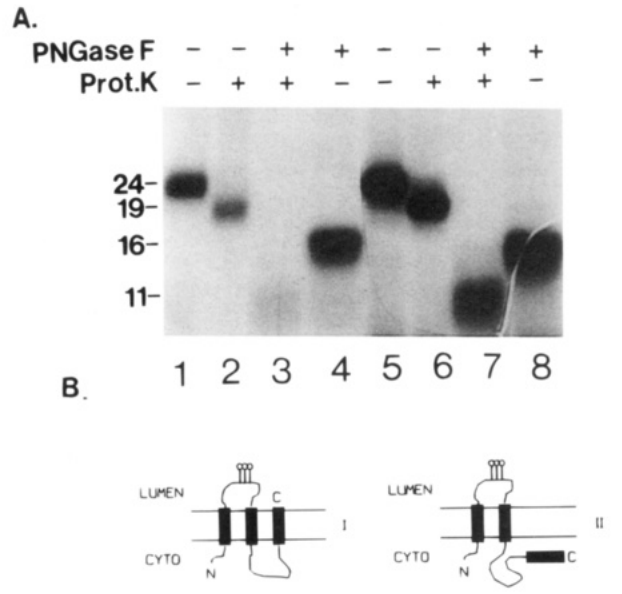

FIGURE 2: The first extracellular loop of Pgp expressed in the RRL or WGE system. (A) *In vitro* translation and posttranslational treatment of *Xho*I-truncated cDNA of Pgp containing the three N-terminal predicted TM segments. *Xho*I-truncated *in vitro* transcripts were used to direct translation in RRL (lanes 1−4) and WGE (lanes 5−8) supplemented with RM. Lanes 2 and 6 are translation products treated with proteinase K. Lanes 3 and 7 are products treated with proteinase K followed by PNGase F. Lanes 4 and 8 are samples treated with PNGase F alone. (B) Possible models of the truncated Pgp. Models I and II are derived from those shown in Figure 1A. The open circles and solid bars indicate the oligosaccharide chains and predicted TM segments, respectively.

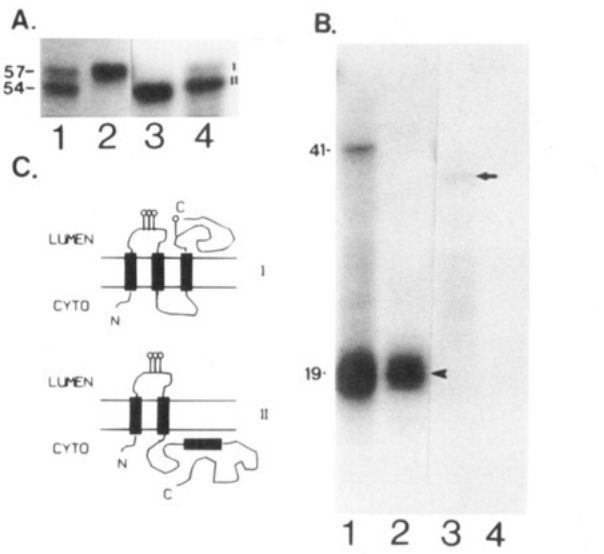

FIGURE 3: Orientation of the predicted TM3 of Pgp translated in the RRL or WGE system. (A) *In vitro* translation of pGPGP-N3 transcripts. Wild-type (lanes 1 and 3) and mutant (lanes 2 and 4) pGPGP-N3 transcripts were used to direct translation in the RRL (lanes 1 and 2) and WGE systems (lanes 3 and 4). I and II indicate the model I (57 kDa) and model II (54 kDa) structures as shown in panel C, respectively. (B) Posttranslational treatment of pGPGP-N3 translation products. WT pGPGP-N3 translation products translated in the RRL (lanes 1 and 3) and WGE systems (lanes 2 and 4) were treated with proteinase K (lanes 1 and 2) and with proteinase K followed by PNGase F (lanes 3 and 4). (C) Topological models of pGPGP-N3 translation products in the membrane. The two models are the same as in Figure 2, except that the molecules in this figure have a C-terminal reporter.

with our previous observation using the RRL translation system (Zhang *et al.*, 1993). Therefore, we conclude that the loop linking the predicted TM1 and TM2 is located in the RM lumen when expressed in both the RRL and WGE translation systems (see Figure 2B).

The Predicted TM3 of Pgp Does Not Reinitiate Membrane Integration in the WGE System. To investigate the membrane orientation of the predicted TM3 in the WGE system, we utilized the previously constructed plasmid pGPGP-N3 (Zhang *et al.*, 1993; see also Figure 1B). This plasmid encodes a truncated Pgp with the N-terminal 3 predicted TM segments (TM1, TM2, and TM3) linked to a C-terminal ATP-binding domain. Both wild-type (WT) and mutant pGPGP-N3 constructs were used in this study. This section addresses only the WT pGPGP-N3, whereas the mutant pGPGP-N3 will be discussed in the next section. Two populations were produced in the RRL system from the WT pGPGP-N3 RNA transcripts [Figure 3C; see also Zhang *et al.* (1993)]. The C-terminal tail of the model I molecule is located in the RM lumen and, therefore, is glycosylated, whereas the C-terminus of the model II molecule is outside of the RM and is not glycosylated. Thus, the model I molecule has a higher molecular weight than the model II molecule. As shown in Figure 3A, RM-associated proteins of 57 and 54 kDa were translated from the pGPGP-N3 transcripts in the RRL system (Figure 3A, lane 1), as previously observed (Zhang *et al.*, 1993). The 57 and 54 kDa proteins represent the model I and II molecules, respectively. When the same transcript was used to direct translation in WGE supplemented with RM, only the 54 kDa model II molecule was produced (Figure 3A, lane 3). As will be described in Figure 4, it is unlikely that the generation of only the 54 kDa protein in the WGE system results from the presence of a protease (see discussion of results in Figure 4D).

To rule out the possibility that the C-terminal reporter of the nascent molecule produced in the WGE system is translocated into the RM lumen but not glycosylated, we performed proteinase K treatment on the RM-associated products. Unglycosylated C-terminal tails in the RM lumen will be protected from proteinase K digestion and a ~39 kDa peptide should be generated. However, a protease-resistant 41 kDa fragment was produced only from the translation product in RRL (Figure 3B, lane 1). This fragment was reduced to a ~39 kDa peptide backbone by endoglycosidase PNGase F digestion (Figure 3B, lane 3) and has been shown to represent the glycosylated C-terminal tail of the model I of pGPGP-N3 translation products (Zhang *et al.*, 1993). Neither the 41 kDa glycosylated fragments nor the 39 kDa peptide backbone was generated from proteinase K digestion of the WGE translation products (Figure 3B, lane 2). Therefore, all nascent pGPGP-N3 translation products in the WGE system have their C-terminal tail on the outside of the RM. These results suggest that the predicted TM3 does not reinitiate membrane translocation in the WGE system. A 19 kDa protease-resistant fragment, predicted from both models I and II, sensitive to PNGase F treatment was also observed in both the RRL and WGE systems (compare lanes 1 and 2 with lanes 3 and 4 in Figure 3B, respectively). It represents the glycosylated loop linking the predicted TM1 and TM2, consistent with the observations shown in Figure 2.

Effect of Arg-207 and Lys-210 on the Predicted TM3-Initiated Membrane Integration. We have shown previously

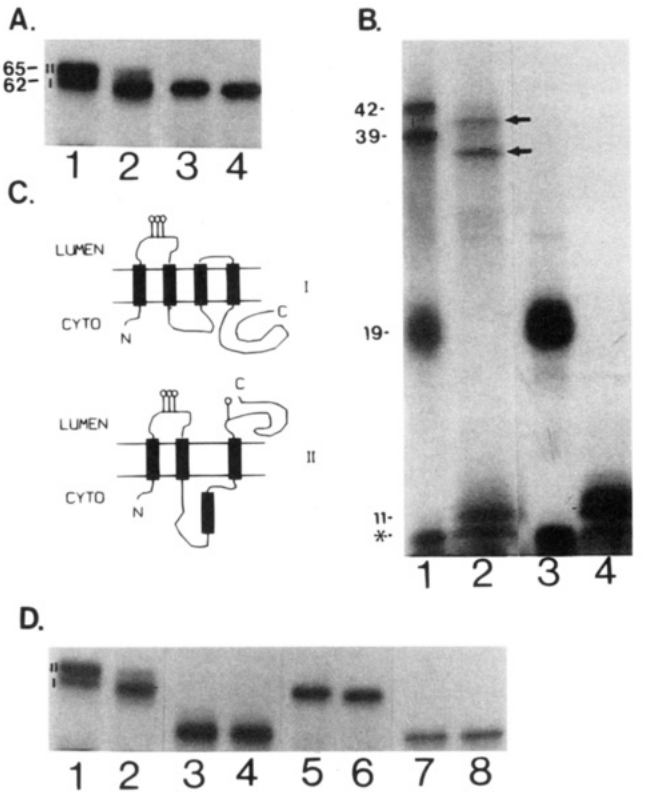

FIGURE 4: Topological orientations of pGPGP-N4 translation products generated in RRL or WGE. (A) *In vitro* translation of WT and mutant pGPGP-N4 transcripts. Wild-type (lanes 1 and 3) and mutant (lanes 2 and 4) pGPGP-N4 transcripts were used to direct translation in RRL (lanes 1 and 2) and WGE (lanes 3 and 4). I and II indicate the models I (65 kDa) and II (62 kDa) structures as shown in panel C, respectively. (B) Posttranslational treatment of pGPGP-N4 translation products. WT pGPGP-N4 translation products translated in RRL (lanes 1 and 2) and WGE (lanes 3 and 4) were treated with proteinase K (lanes 1 and 3) and with proteinase K followed by PNGase F (lanes 2 and 4). (C) Topological models of pGPGP-N4 translation products. The two models are the same as those described in Figure 1A, except that there are only four predicted TM segments and a reporter peptide for pGPGP-N4 translation products. (D) PNGase F treatment of the WT and mutant PGP-N4 translation products. Membrane-associated WT and mutant PGP-N4 molecules translated in RRL (lanes 1−4) and WGE (lanes 5−8) were treated with PNGase F (lanes 3, 4, 7, and 8) or without PNGase F (lanes 1, 2, 5, and 6). Lanes 1, 3, 5, and 7 are WT, whereas lanes 2, 4, 6, and 8 are mutant. Clearly, the peptide backbones of both WT and mutant PGP-N4 molecules translated in RRL and WGE have the same size.

that mutation of Arg-207 and Lys-210 to Val and Asp, respectively, at the C-terminus of the predicted TM3 converted all translation products of pGPGP-N3 transcripts into the model I orientation in the RRL system (Zhang *et al.*, 1995; see also Figure 3A, lane 2, and Figure 3C). When the same mutant pGPGP-N3 transcript was used to direct translation in WGE, a significant fraction of the mutant translation product was found to have the model I orientation (Figure 3A, lane 4), whereas no model I molecules were generated from the WT pGPGP-N3 transcript (Figure 3A, lane 3). A ~41 kDa protease-resistant fragment was produced upon proteinase K digestion of the mutant pGPGP-N3 translation products in the WGE system (data not shown), confirming that some mutant pGPGP-N3 translation products were in the model I orientation. We conclude that the positively charged amino acids at the C-terminus of the predicted TM3 play an important role in TM3-initiated membrane translocation in both systems. Thus, the mutation can convert the pGPGP-N3 translation products from model II to model I structure in the WGE system, although with a lower efficiency than in the RRL system.

Topology of the Predicted TM4 of Pgp Translated in the WGE or RRL System. To determine whether the membrane integration of the predicted TM4 is also different in both translation systems, we used the pGPGP-N4 construct in the RRL and WGE systems. The pGPGP-N4 construct encodes a truncated Pgp containing the four amino-terminal predicted TM segments linked to a C-terminal ATP-binding domain reporter as previously described (Zhang *et al.*, 1993; see also Figure 1B). Two major products of 65 and 62 kDa were translated from the pGPGP-N4 transcript in the RRL system (Figure 4A, lane 1; Zhang *et al.*, 1993). These two products represent molecules with model II and model I orientations (Figure 4C), respectively. The model II molecules have an extra oligosaccharide chain, accounting for their slower mobility on SDS−PAGE. They are presumably produced by a TM4-initiated membrane translocation and glycosylation of the C-terminal sequence (Zhang *et al.*, 1993; Figure 4C).

In the WGE system, however, only the 62 kDa protein was produced from the pGPGP-N4 RNA transcript (Figure 4A, lane 3). Therefore, it is likely that the predicted TM4 does not initiate membrane integration to translocate its C-terminal sequence into the RM lumen, and only model I topology is observed. Treatment with proteinase K generated a 42 kDa protease-resistant fragment from the pGPGP-N4 translation products in the RRL system (Figure 4B, lane 1), but not from those translated in the WGE system (Figure 4B, lane 3). This result indicates that the 62 kDa protein in the WGE system represents a model I molecule and not a model II molecule with an unglycosylated C-terminal tail in the RM lumen. The 39 kDa protease-resistant fragment is an internally initiated translation product that has been translocated into the RM lumen in RRL (Figure 4B, lane 1; Zhang *et al.*, 1993). It is a translation product initiated at ATG-683 that has a Kozak consensus sequence. Both the 39 and 42 kDa fragments are glycosylated, as demonstrated by PNGase F treatment (Figure 4B, lane 2). These results are consistent with our previous observations (Zhang *et al.*, 1993). Furthermore, pGPGP-N4 translation products in both the RRL and WGE systems generated a 19 kDa protease-resistant fragment of the first extracellular loop that can be reduced to ~11 kDa (Figure 4B, lanes 2 and 4). It is not known why a doublet of 11 kDa products was produced in the WGE system. This is possibly due to incomplete proteinase K digestion. Another protease-resistant fragment observed in both systems has an apparent size of ~10.5 kDa (Figure 4B, lanes 1 and 3) and resists digestion by PNGase F (Figure 4B, lanes 2 and 4). It was not observed with the pGPGP-N3 translation products (data not shown) and probably represents the membrane-protected TM3−loop−TM4 fragment. The mutant R207N (Zhang *et al.*, 1993), which reduced the generation of model II pGPGP-N4 translation products in RRL (compare lanes 1 and 2 in Figure 4A), apparently did not affect the generation of model I molecules in the WGE system (compare lanes 3 and 4 in Figure 4A).

To rule out the possibility that the WGE system contains a protease that is responsible for the generation of only the small size proteins (54 kDa PGP-N3 and 62 kDa PGP-N4 molecules), we performed an experiment to test the size of the peptide backbone of the PGP-N4 proteins generated in the RRL and WGE systems. If the 62 kDa protein produced

in the WGE system represents a proteolyzed version of the 65 kDa protein generated in RRL, complete removal of sugars will reveal the difference in size of the peptide backbones generated in both systems. However, as shown in Figure 4D, endoglycosidase PNGase F digestion of membrane-associated pGPGP-N4 translation products in RRL (lanes 3 and 4) and WGE (lanes 7 and 8) showed that both the wild-type (lanes 3 and 7) and the mutant (lanes 4 and 8) peptide backbones have the same size regardless of the translation system used. The samples in lanes 1 and 2 and lanes 5 and 6 are products translated in RRL and WGE, respectively, and are controls treated without PNGase F.

WGE Contains a Dominant Activity That Inhibits TM3- and TM4-Initiated Membrane Integration. The preceding studies suggest that there may be cytoplasmic factors in WGE that inhibit TM3- and TM4-initiated membrane integration. Alternatively, RRL may contain factors that activate TM3- and TM4-initiated membrane integration. To differentiate between these two possibilities, we carried out experiments in which different amounts of RRL and WGE were premixed, and the pGPGP-N3 and pGPGP-N4 transcripts were then added to initiate translation and membrane translocation. As shown in Figure 5A, generation of the model I structure of pGPGP-N3 and the model II structure of pGPGP-N4 translation products decreases as the WGE fraction increases. These structures disappear from the translation mixtures containing 20% or more of WGE. These results suggest that the WGE contains one or more factors that inhibit TM3- and TM4-initiated membrane integration.

The Inhibitory Activity in WGE Is Soluble, Heat-Labile, and Trypsin-Sensitive. We next determined whether the dominant inhibitory activity in WGE is associated with the ribosomal or the soluble fraction. The ribosomal and soluble cytoplasmic fractions of WGE were separated by ultracentrifugation. An approximately equal portion of either the ribosomal or soluble fraction was mixed with the RRL to a final concentration of ~10% (vol/vol) before the *in vitro* transcripts were added to initiate translation at 30 °C for 90 min. Membrane-associated translation products were analyzed by SDS−PAGE. As shown in Figure 5B, the generation of the model I pGPGP-N3 and model II pGPGP-N4 translation products was inhibited by the supernatant fraction of WGE (lanes 5 and 11). The pellet fraction may also have some minor inhibitory effects (lanes 3 and 9), but this may be due to cross-contamination by the supernatant fraction. The supernatant fraction also appears to inhibit the overall translation efficiency (lanes 5 and 11). When the active fractions were boiled for 2 min before being added to the translation, they lost their inhibitory effects upon the generation of the model I pGPGP-N3 (lanes 4 and 6) and model II pGPGP-N4 (lanes 10 and 12) translation products. These results suggest that the inhibitory activity observed in the WGE is likely soluble proteins.

To confirm that the inhibitory activity associated with WGE is by large molecules such as proteins rather than small molecules such as ions, WGE was stripped of low molecular weight components using a Sephadex G-50 spin column, and the excluded fraction was collected. The column was then washed twice with H_2O and the included fractions were collected. As before, each individual fraction was then mixed with RRL to a final concentration of ~10% (vol/vol), and the translation was initiated by pGPGP-N4 transcripts at 30 °C for 90 min. Membrane-associated translation products were analyzed by SDS−PAGE. As shown in Figure 5C, the generation of the model II molecules from pGPGP-N4 transcript was inhibited by the excluded fraction (lane 2) to a similar extent as by unfractionated WGE (lane 1). The two following included wash fractions did not have any inhibitory effect on the generation of model II products of the pGPGP-N4 transcripts (lanes 3 and 4), similar to the H_2O control (lane 5). Therefore, the inhibitory activity in

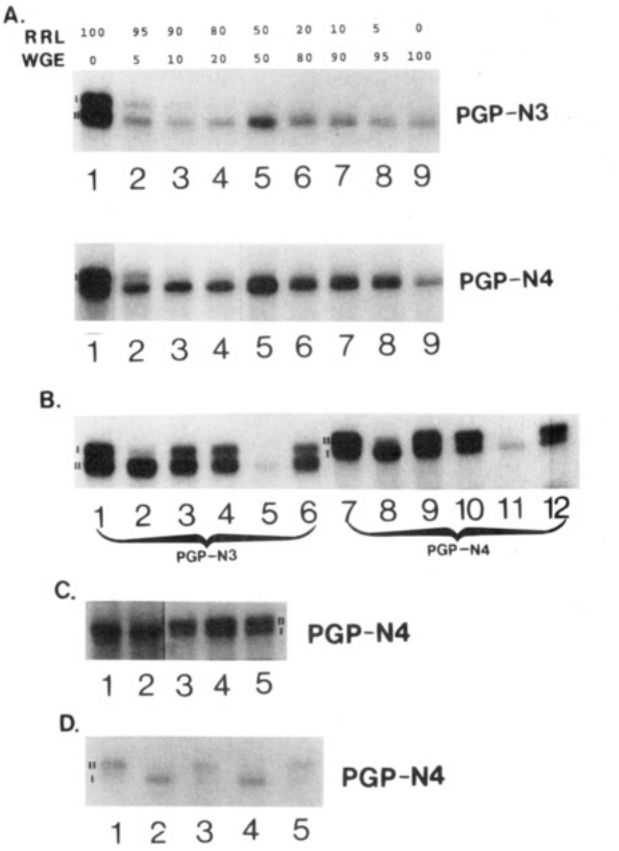

FIGURE 5: Inhibition of TM3- and TM4-initiated membrane insertion by WGE fractions. (A) Unfractionated WGE inhibits the generation of model I pGPGP-N3 and model II pGPGP-N4 translation products in the RRL system. Various amounts of WGE and RRL were premixed before the addition of pGPGP-N3 or pGPGP-N4 RNA to induce translation. Two molecules representing models I and II were generated in the pure RRL translation system (lane 1), whereas only one was generated in the pure WGE system (lane 9). The numbers on top indicate the percent fraction of RRL and WGE in each translation. (B) The inhibitory activity in WGE is associated with a soluble and heat-labile fraction. Translation in RRL was induced by pGPGP-N3 (lanes 1−6) and pGPGP-N4 (lanes 7−12) RNA in the absence (lanes 1 and 7) or presence of 10% WGE (lanes 2 and 8), insoluble WGE (lanes 3 and 9), boiled insoluble WGE (lanes 4 and 10), soluble WGE (lanes 5 and 11), and boiled soluble WGE (lanes 6 and 12). (C) The inhibitory activity in WGE is excluded from Sephadex G-50. The size of the WGE fraction with inhibitory activity was estimated by using the Sephadex G-50 column, and the activity of each fraction was tested by initiating translation of pGPGP-N4 RNA in RRL in the presence of WGE (lane 1), excluded fraction (lane 2), two included fractions from 50 μL washes with H_2O (lanes 3 and 4), and H_2O control (lane 5). (D) The inhibitory activity in WGE is sensitive to trypsin digestion. To determine whether the WGE fraction is a protein, a soluble fraction of WGE was treated with insoluble trypsin, and the post-trypsin fraction was added before translating pGPGP-N4 RNA in RRL (lanes 3 and 5). Lanes 2 and 4 are controls with the addition of a WGE fraction treated without trypsin. Lane 1 is a control with H_2O added. Lanes 2 and 3 are duplicate experiments of lanes 4 and 5.

WGE is attributable to high molecular weight components, possibly proteins.

To further study the nature of the inhibitory factor in WGE, the soluble fraction of WGE was trypsinized and mixed with RRL to a final concentration of ~10% (vol/vol) before translation was initiated with pGPGP-N4 RNA. As shown in Figure 5D, the generation of model II molecules from the pGPGP-N4 transcript was inhibited by the soluble fraction of the WGE (Figure 5D, lanes 3 and 5). However, the ability to generate model II molecules from the pGPGP-N4 transcript was not inhibited by the trypsinized WGE soluble fraction (Figure 5D, lanes 2 and 4). Lane 1 is a control reaction with H_2O added. These results indicate that the inhibitory fraction in WGE is likely composed of protein(s). However, it should be noted that the inhibition of the translation efficiency observed in RRL by WGE was not recovered by trypsin treatment of WGE. The amount of samples loaded in lanes 2−5 is equivalent to 8-fold that loaded in lane 1. Apparently, the putative factors causing the slow translation rate and the factor causing the generation of only one topology of Pgp are different.

DISCUSSION

The aim of this paper was to investigate whether the cytoplasmic components of a cell-free translation system contain factors capable of regulating different topological structures of truncated Pgp molecules. The main conclusion is that the WGE contains a fraction absent from the RRL that inhibits TM3- and TM4-initiated membrane translocation. This fraction is soluble, heat-labile, excluded from Sephadex G-50, sensitive to trypsin, and probably consists of one or more proteins. This fraction is relatively stable since it is insensitive to repeated freeze-thawing (unpublished observation). It is interesting to note that, in contrast to the present study, a heat-labile cytoplasmic component in RRL not present in WGE has been shown to be involved in regulating the generation of secretory forms of prion proteins (Lopez *et al.*, 1990). Thus, it is possible that specific cytoplasmic factors are involved in regulating the expression of different topological structures of some polytopic membrane proteins in mammalian cells.

This study, together with our previous findings (Zhang *et al.*, 1995), suggests that in the WGE there are at least two topological determinants of Pgp sequence: (1) cytoplasmic heat-labile and trypsin-sensitive factors and (2) an internally localized amino acid sequence of Pgp. The heat-labile and trypsin-sensitive cytoplasmic factors in the WGE characterized in this study appear to allow only the coinsertion of the predicted TM3 and TM4 into the lipid bilayer of the membrane, but not any single insertion by the predicted TM3 or TM4 of the truncated Pgp molecules. It is tempting to speculate that these factors function as transmembrane-binding factors (TMBF) that bind and prevent the nascent predicted TM3 and TM4 of Pgp from integrating into the membrane alone. Binding of TMBF to the predicted TM3 of pGPGP-N3 translation products will prevent the TM3 from integrating into the membrane, resulting in only the model II topology (Figure 3C). Binding of TMBF to the predicted TM4 of pGPGP-N4 translation products will also prevent the membrane integration of TM4, and therefore, no model II topology is produced (Figure 4C). In the latter case, these factors may function as a foldase (Lingappa, 1991) and convert the predicted TM3 and TM4 into a membrane translocation-competent pair. This folding process results in the generation of only the model I topology of pGPGP-N4 translation products. It is noteworthy that the translation efficiency of truncated Pgp molecules in WGE is lower than that in RRL, and the soluble fraction of WGE also lowers the translation efficiency in RRL. It is not known whether WGE contains any factor that slows the translation rate, which in turn affects the folding of truncated Pgp molecules. However, two topologies of Pgp were generated in RRL in the presence of trypsinized WGE, whereas the translation rate did not recover by trypsin treatment of the WGE (see Figure 5D). Furthermore, slowing of the translation rate in RRL by reducing the amount of RNA template in the translation did not eliminate the generation of the alternate topology of Pgp (unpublished observation). Therefore, it is unlikely that the slow translation rate *per se* is responsible for the generation of only one topology of Pgp in WGE.

In the RRL system, these presumptive TMBF presumably are not present, and the membrane insertion of the predicted TM3 and TM4 appears to be modulated by the amino acids surrounding these predicted TM segments; therefore, two orientations can occur (Figures 3C and 4C). It is worth noting that the membrane insertion of the predicted TM1 and TM2 of Pgp is not affected by the heat-labile and trypsin-sensitive factors. It is possible that the postulated TMBF bind to only the predicted TM3 and/or TM4 of the truncated Pgp molecules. Skach and Lingappa (1994) recently reported that the predicted TM3 and TM4 of human *MDR1* Pgp expressed in frog oocytes translocate across the membrane only twice. This is different from our previous study, which showed that the predicted TM3 and TM4 of hamster *pgp1* Pgp span the membrane either once or twice (Zhang *et al.*, 1993). This difference may be due to the expression of particular TMBF in frog oocytes. Therefore, it is predicted that expression of the predicted TM3 and TM4 of Pgp in frog oocytes will generate a topological structure similar to that expressed in the WGE system. The observation by Bibi and Beja (1994) that the predicted TM3 of mouse *mdr1* Pgp is located in the membrane and the predicted TM4 is found in extracellular space may also result from the involvement of particular TMBF in bacteria. Since Skach *et al.* (1993) also reported that the C-terminal half molecules expressed in oocytes and in the RRL system have the same structure, it is possible that the TMBF involved in the regulation of the N-terminal half topology do not regulate the membrane orientation of the C-terminal half of Pgp. It will be of interest to determine whether heat-labile cytoplasmic components analogous to these found in WGE are expressed in mammalian cells.

The presence of two positive charges (Arg-207 and Lys-210) in the loop between predicted TM3 and TM4 inhibits the generation of the model I structure of truncated Pgp molecules (Figures 3C and 4C). Mutation of these two amino acids to neutral or negatively charged residues decreased this inhibitory effect and facilitated the generation of the model I structures. These mutations can only partially overcome the inhibitory effect of the postulated TMBF on the predicted TM3 of pGPGP-N3 translation products. However, these mutations, as well as the postulated TMBF, facilitate the generation of model I structure of pGPGP-N4 translation products. Previously, it has been suggested that

endoplasmic reticulum (ER) contains protein-conducting channels involved in membrane protein biogenesis (Simon & Blobel, 1991). These channels may interact with the charged amino acids of Pgp and function as a receptor for the postulated TMBF in regulating the generation of different topologies.

Results in the current study indicate that the topology of a polytopic membrane protein can vary greatly in different *in vitro* expression systems. Previously, Spiess *et al.* (1989) observed that the stop-transfer activity of some hydrophobic sequences of engineered asialoglycoprotein receptor H1 behave differently in WGE and RRL, and the RRL appears to reflect the situation in NIH-3T3 fibroblast cells. By analogy, we speculate that hamster *pgp1* Pgp expressed in different cell types may have different structures and that these differences are perhaps responsible for its variable functions. It will be of great interest to determine whether the alternative topologies of Pgp identified *in vitro* are also expressed in mammalian cells *in vivo*.

ACKNOWLEDGMENT

The authors thank Drs. Karl Karnaky, Jr., Javior Navarro, and Luis Reuss for their critical comments on the manuscript. The authors also thank their colleagues at OCI and UTMB for their helpful discussions.

REFERENCES

Bear, C. E. (1994) *Biochem. Biophys. Res. Commun. 200*, 513–521.

Bibi, E., & Beja, O. (1994) *J. Biol. Chem. 269*, 19910–19915.

Childs, S., & Ling V. (1994) *Important advAnces in Oncology* (DeVita, V., Hellman, S., & Rosenberg, S., Eds.) J. B. Lippincott Company, Philadelphia.

Endicott, J. A., & Ling, V. (1989) *Annu. Rev. Biochem. 58*, 137–171.

Gafvelin, G., & von Heijne, G. (1994) *Cell 77*, 401–412.

Gottesman, M. M., & Pastan, I. (1993) *Annu. Rev. Biochem. 624*, 385–427.

Higgins, C. F. (1992) *Annu. Rev. Cell Biol. 8*, 67–113.

Lingappa, V. R. (1991) *Cell 65*, 527–530.

Lopez, C. D., Spencer, Y., Prusiner, S. B., Myers, R. M., & Lingappa, V. R. (1990) *Science 248*, 226–229.

Meyer, D. I., Krause, E., & Dobberstein, B. (1982) *Nature 297*, 647–650.

Sharma, R. C, Inuoe, S., & Roitelman, J. (1992) *J. Biol. Chem. 267*, 5731–5734.

Simon, S. M., & Blobel, G. (1991) *Cell 65*, 371–380.

Skach, W. R., & Lingappa, V. R. (1994) *Cancer Res. 54*, 3202–3209.

Skach, W. R., Calayag, M. C., & Lingappa, V. R. (1993) *J. Biol. Chem. 268*, 6903–6908.

Spiess, M., Handschin, C., & Baker, K. P. (1989) *J. Biol. Chem. 264*, 19117–19124.

Walter, P., Ibrahimi, I., & Blobel, G. (1981) *J. Cell Biol. 91*, 545–550.

Zhang, J. T., & Ling, V. (1991) *J. Biol. Chem. 266*, 18224–18232.

Zhang, J. T., Duthie, M., & Ling, V. (1993) *J. Biol. Chem. 268*, 15101–15110.

Zhang, J. T., Lee, C. H., Duthie, M., & Ling, V. (1995) *J. Biol. Chem. 270*, 1742–1746.

BI9425664